THE ASTROPHYSICAL JOURNAL, 314:726–738, 1987 March 15

THE "SEI" METHOD FOR ACCURATE AND EFFICIENT CALCULATIONS OF LINE PROFILES IN SPHERICALLY SYMMETRIC STELLAR WINDS

H. J. G. L. M. LAMERS
SRON Laboratory for Space Research; and Sonnenborgh Observatory, Utrecht
M. CERRUTI-SOLA
Osservatorio Astrofisico di Arcetri
AND
M. PERINOTTO
Istituto di Astronomia, Università di Firenze; and European Southern Observatory
Received 1986 April 3; accepted 1986 August 26

ABSTRACT

A fast and accurate method for calculating line profiles in stellar winds is described. The method is based on the calculation of the source function with the escape probability method with a calculation of an exact solution of the transfer equation. The method allows the calculation of singlets and doublets with underlying photospheric absorption components. A comparison with profiles calculated with the Sobolev approximation shows excellent agreement if the velocities of the chaotic motions in the wind are small ($<0.02v_\infty$). For larger turbulent velocities, the deviation from the Sobolev approximation is quite significant. A comparison with profiles calculated with the comoving-frame method shows very good agreement for both optically thin and thick lines. Our method slightly underestimates the amount of emission in very optically thick lines. The simplicity and accuracy of the method allows the efficient use of spectra for interactive analysis. A number of profiles calculated for various physical conditions in the wind are shown. The presence of turbulence in the winds of Wolf-Rayet stars will result in almost symmetric profiles which are redshifted by at most 2.5 times the turbulent velocity.

Subject headings: line profiles — radiative transfer — stars: winds

I. INTRODUCTION

The structure of stellar winds and the mass loss from stars can be studied from the line profiles. These profiles can be either in emission, e.g., in the spectra of Wolf-Rayet stars; in absorption with extended violet wings, e.g., in the UV spectrum of late O and early B main-sequence stars; or P Cygni–type profiles, e.g., in the UV spectra of OB supergiants. From a comparison of the observed profiles and the calculated profiles, one can derive the column density of the observed atoms and their distribution as a function of velocity and the velocity law. This information can then be used to derive the mass loss rate.

After the first quantitative studies of winds based on the *Copernicus* observations of ζ Pup and τ Sco by Lamers and Morton (1976) and Lamers and Rogerson (1978), many mass loss studies based on the fitting of the UV line profiles have appeared in the literature (e.g., Conti and Garmany 1980; Garmany *et al.* 1981; Gathier Lamers, and Snow 1981; Olson and Castor 1981; Prinja and Howarth 1985). In these studies the line profiles were calculated with the Sobolev method, which is valid if the velocity gradient in the wind, dv/dr, is larger than v_t/l, where v_t is the combined thermal and turbulent velocity of the ions and l is the characteristic length in the wind over which the density or the ionization changes. In that case the line absorption coefficient can be approximated by a delta function in the frequency, because its intrinsic width can be neglected. This implies that the radiative transfer can be simplified in two ways: the source function depends only on the local conditions, and the transfer equation can be solved analytically because τ increases as a step function.

The Sobolev approximation is a reasonable assumption for the study of the rapidly accelerating winds of early-type stars, which reach velocities of ~ 2000 km s^{-1} in a few stellar radii. The results derived by this method are reasonably accurate, i.e., within $\sim 25\%$, for the accelerating part of the wind if the lines are not saturated. However, when the lines are strong and reach depths of 90% or more, or when the winds are turbulent, with v_t larger than $\sim 1/10$ the terminal wind velocity, much larger errors are to be expected. The major advantage of the Sobolev method and the reasons that it has been used extensively is its simplicity and efficiency, which allows the observers to use this method interactively in the fitting of calculated profiles to the observations.

An alternative and very accurate method for calculating line profiles in moving atmospheres is the comoving-frame method (CF) developed by Mihalas, Kunasz, and Hummer (1975) and used extensively by Hamann (e.g., 1980, 1981*a*). The advantage of the CF method is that it is very accurate and can be used for atmospheres with small velocity gradients. However, it cannot be used efficiently for interactive spectral analysis.

As more accurate observations become available and the studies of stellar winds require more detailed analysis, there is a need for an accurate and efficient method of profile calculation. The requirements for such a method are the following: (*a*) it must be able to take into account the presence of turbulence or other chaotic motions in the accelerating wind, (*b*) it must be accurate up to large optical depths, (*c*) it must be able to calculate the line transfer for doublets, (*d*) the presence of underlying photospheric components must be treated in the transfer equation, and (*e*) the calculation of line profiles should be fast enough to be used interactively with medium-size computers.

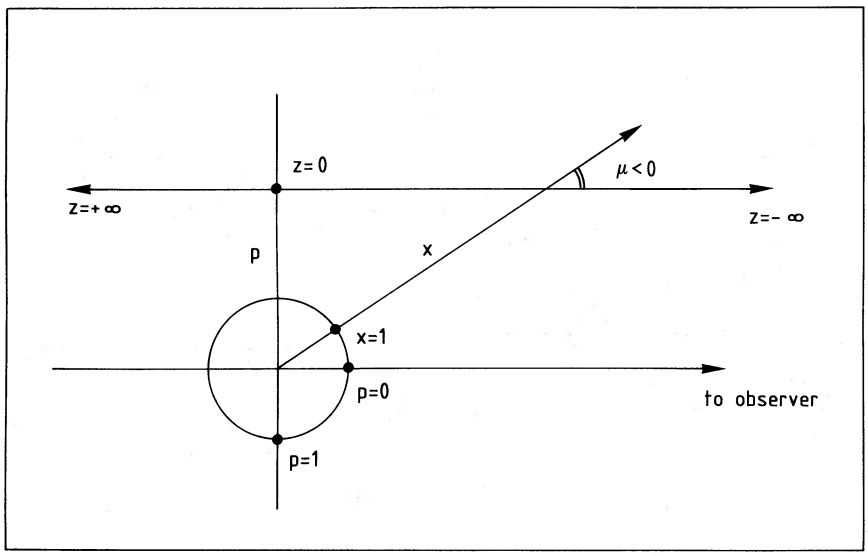

FIG. 1.—Coordinate system adopted in this paper. All distances, x, p, and z, are normalized to $R_* = 1$.

The method described in this paper satisfies all the above-mentioned requirements. It is based on a suggestion by Hamman (1981*a*), who pointed out that the source function calculated by the Sobolev approximation is accurate for a large range of physical conditions in stellar winds. He showed that most of the errors of the Sobolev line profiles are due to the step function assumed in the solution of the transfer equation.

In our method (Sobolev with exact integration, hereafter SEI), the source function is calculated in the Sobolev approximation, but the equation of transfer is solved exactly. It was developed while one of us (H. J. G. L. M. L.) was a guest of the Osservatorio Astrofisico di Arcetri, Firenze.

In §§ III and IV the SEI method for calculating the profiles of singlets and doublets is described. The results are compared in § V with those obtained by the Sobolev method and the comoving frame method. In § VI we present some results of P Cygni profiles and emission line profiles.

II. THE COORDINATE SYSTEM

Throughout this paper we use the coordinate system shown in Figure 1. The coordinates are: distances from the star x, impact parameter for the line of sight p, and distance along the line of sight z, all normalized to the stellar radius. The angle between the line of sight and the radial vector is arccos μ, with $\mu = 1$ if the radial vector points to the observer. For any point in the wind x, p and z are related by

$$z = \mu x = \mu(p^2 + z^2)^{1/2} . \tag{1}$$

Throughout this paper all velocities are expressed in non-dimensional units $w = v/v_\infty$ which are normalized to the terminal velocity v_∞ of the wind. In most cases the frequencies are also expressed in terms of w by means of

$$w = (\nu - \nu_0)c/(\nu_0 v_\infty) , \tag{2}$$

where ν_0 is the rest frequency of the line. The velocity law can thus be written as $w(x)$, and the radial velocity as seen by the observer is $w_z = \mu w(x)$. This implies that the velocity gradient along a line of sight specified by p is

$$\frac{dw_z}{dz} = \left[1 + \mu^2\left(\frac{x}{w}\frac{dw}{dx} - 1\right)\right]\frac{w(x)}{x} . \tag{3}$$

III. THE SEI METHOD FOR SINGLE LINES

The SEI method is based on the assumption that the source function in a rapidly expanding atmosphere can be calculated with reasonable accuracy by means of the escape probability method, but that the transfer equation should be solved accurately. This allows us to calculate line profiles formed in a spherically symmetric expanding wind with a monotonically increasing velocity law, in which chaotic motions act as "turbulence." The profile of the turbulence can be specified, e.g., by a Gaussian profile with an outward increasing or decreasing width. The turbulence can be treated as "spherical, i.e., having the same distribution in all directions, but it can also be treated as a "one-dimensional" turbulence, e.g., in the radial direction only. This radial turbulence can mimic the occurrence of small length-scale perturbations of the velocity law.

The radiative transfer equation is solved in the wind only. The photosphere is considered as a lower boundary condition. Its spectrum is a continuum with or without an absorption line at the rest frequency of the line whose profile is to be calculated. This photospheric profile has to be specified. Photospheric limb darkening is neglected, since its effect on the P Cygni profiles formed in the wind is negligible (Castor and Lamers 1979).

The artificial separation between the photosphere and the wind can produce errors in the predicted profiles close to the line center (see Hamman 1981*a*). Since the physical conditions in the transition layers between the photosphere and the wind are not very well known, the errors produced by our method are not expected to hamper the analysis of stellar spectra significantly. But if the conditions near the base of the wind are of interest, one should use the CF method.

a) The Source Function

The source function in a two-level atom can be written as

$$S_\nu(x) = [\beta_c(x) I_\nu^* + \epsilon' B_\nu(x)]/(\beta + \epsilon') , \tag{4}$$

where I_ν^* is the intensity at frequency ν of the radiation leaving the stellar photosphere, B_ν the Planck function in the wind, and $\epsilon' = C_{ul}/A_{ul}$ is the ratio of collisional to radiative deexcita-

tions. In this expression β is the escape probability for line photons

$$\beta(\tau_0, \sigma) = \int_0^1 \left(\frac{1+\sigma\mu^2}{\tau_0}\right)\left[1 - \exp\left(-\frac{\tau_0}{1+\sigma\mu^2}\right)\right]d\mu , \quad (5)$$

and β_c is the penetration probability for continuum photons

$$\beta_c(\tau_0, \sigma, z) = \frac{1}{2}\int_{\mu_c}^1 \left(\frac{1+\sigma\mu^2}{\tau_0}\right)\left[1 - \exp\left(-\frac{\tau_0}{1+\sigma\mu^2}\right)\right]d\mu \quad (6)$$

where

$$\sigma = \frac{x}{w}\frac{dw}{dx} - 1 , \quad (7)$$

and $\mu_c = (1 - z^2)^{1/2}$ (Castor 1970). The optical depth in the above expression is defined as

$$\tau_0(x) = \frac{\pi e^2}{mc}(gf)_{lu}\left(\frac{n_l}{g_l} - \frac{n_u}{g_u}\right)\frac{R_*}{v_\infty}\frac{c}{v_0}\frac{x}{w} . \quad (8)$$

For resonance lines $n_u/g_u \ll n_l/g_l$, and one can approximate

$$\tau_0(x) \approx \frac{\pi e^2}{mc} f\lambda_0 n_i \frac{x}{w}\frac{R_*}{v_\infty} , \quad (9)$$

where n_i is the number of ions per cm^3.

For a multilevel atom, the source function can be written in an "equivalent two-level atom" expression

$$S_\nu(x) = [\beta_c(x)I_\nu^* + (\epsilon' + \theta)B_\nu(x)]/(1 + \epsilon' + \eta) , \quad (10)$$

where θ and η allow for the coupling to other levels (see Mihalas 1978, p. 377).

If the photospheric spectrum contains a continuum I_c with an absorption line, then

$$I_\nu^* = I_c[1 - A(\nu - \nu_0)] , \quad (11)$$

where A is the absorption. The intensity at distance x, frequency ν_0, and angle μ is

$$I_{\nu_0}(x, \mu) = I_c[1 - A(\Delta\nu')] , \quad (12)$$

with $\Delta\nu' = \nu_0 v_\infty w(x)\mu/c$. The escape probability β_c, which describes the contribution of the continuum photons to the mean intensity $\bar{J}_\nu$, becomes

$$\beta_c(\tau_0, \sigma, z) = \frac{1}{2}\int_{\mu_c}^1 [1 - A(\Delta\nu')] \times \left(\frac{1+\sigma\mu^2}{\tau_0}\right)\left[1 - \exp\left(\frac{-\tau_0}{1+\sigma\mu^2}\right)\right]d\mu , \quad (13)$$

whereas β remains as before.

b) *The Solution of the Transfer Equation*

The solution of the transfer equation gives the intensity as seen by an observer at a line of sight p:

$$I_\nu(p) = \int_{z=-\infty}^{z=\infty} S_\nu(z')e^{-\tau_\nu(z')}d\tau_\nu(z') , \quad \text{for } p \geq 1 , \quad (14)$$

$$= \int_{z=-\infty}^{-z_*} S_\nu(z')e^{-\tau_\nu(z')}d\tau_\nu(z') + I_\nu^* e^{-\tau_\nu(-z_*)} , \quad \text{for } p < 1 . \quad (15)$$

The second equation describes the intensity coming from the line of sight which intersects the star at $z = -z_* = -(1 - p^2)^{1/2}$ and contains a contribution from the photospheric radiation I_ν^*, which is described by equation (11) if the photospheric spectrum contains an absorption line.

The optical depth in the expression for $I_\nu(p)$ is

$$\tau_\nu(z') = \int_{-\infty}^{z'} \tau_0(x)\Phi_\nu(z)/(1 + \sigma\mu^2)dz \quad (16)$$

(Castor 1970), where the integration should be made along a line of of sight of contant p. In this expression the profile function $\Phi_\nu(z)$ is determined by the local turbulence in the wind. If ϕ is expressed in terms of the dimensionless velocity w,

$$\phi(\Delta\omega) = \pi^{-1/2}w_D^{-1} \exp[-(\Delta w/w_D)^2] , \quad (17)$$

with $w_D^2 = w_T^2 + w_t^2$, where $w_T = v_{\text{turb}}/v_\infty$ and $w_t = v_{\text{thermal}}/v_\infty$, then $\Phi_\nu(z)$ is defined by

$$\Phi_\nu(z) = \phi\left[\Delta w = \mu w(x) - \frac{\nu - \nu_0}{\nu_0}\frac{c}{v_\infty}\right]\frac{dw_Z}{dz} , \quad (18)$$

where z and x are coupled by the condition that p is constant.

Equations (14) and (15) describe $I_\nu(p)$. The flux, normalized to the continuum, is

$$F_\nu = \int_0^\infty [I_\nu(p)/I_c]2pdp . \quad (19)$$

The integration scheme for the calculation of I is shown in Figure 2.

IV. THE SEI METHOD FOR DOUBLET LINES

Many interesting spectral lines consist of doublets, whose profiles formed in an expanding atmosphere overlap one another. In this case the solution of the radiative transfer problem is considerably more complicated than in the case of a single line, since photons which are scattered or emitted by one of the components may interact at another place in the wind with the other component. This implies that the source function of one component is affected by the presence of the other component, because the latter will contribute to the radiation field as seen by the first component. In a spherically expanding wind with a monotonically increasing velocity law, all atoms are moving away from one another. For this reason a photon which is emitted or scattered by the red component of the doublet cannot be absorbed again in the wind by the blue component. On the other hand, a photon emitted or scattered by the blue component can be absorbed elsewhere in the wind by the red component, but only by an atom whose velocity relative to the emitting atom corresponds exactly to the wavelength difference between the two doublets. For this reason the source function of the red component will be affected by the presence of a blue component, but not vice versa.

In this paper we refer to the two components as the blue (subscript B) and red (subscript R) components respectively. The separation of the doublets in terms of the normalized velocity is δ;

$$\delta = (v_B - v_R)c/v_B v_\infty . \quad (20)$$

Surdej (1980) and Olson (1982) have described a method for calculating doublets in an expanding wind in the Sobolev approximation with the escape probability method which follows the analysis of Rybicki and Hummer (1978) for general nonlocal coupling within the Sobolev approximation. We adopt Olson's method for the calculation of the source func-

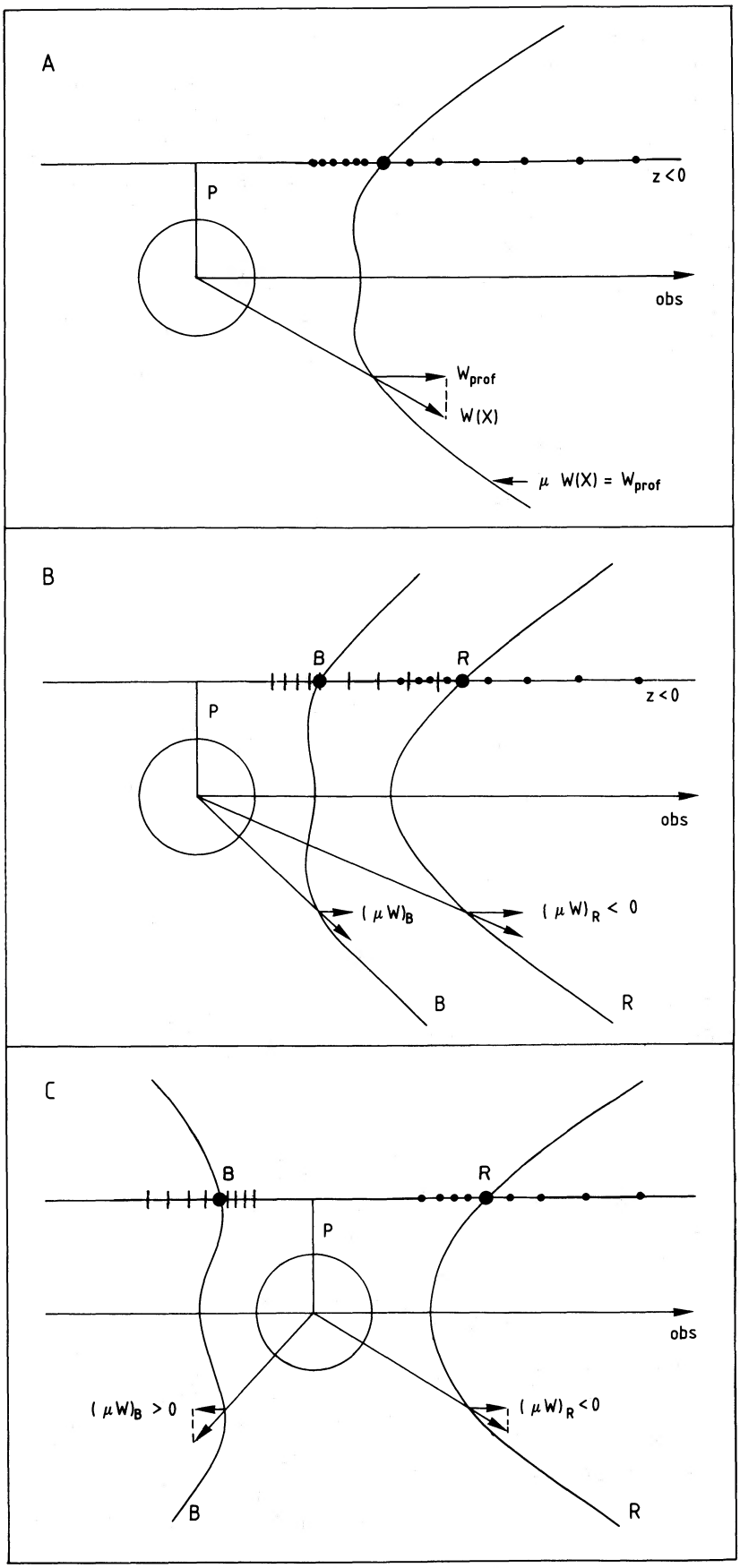

FIG. 2.—Scheme used for the integration of the emergent intensity $I_\nu(p)$ along a line of sight with impact parameter p. The points used for the numerical integration of τ and I are shown by circles and vertical marks on the line of sight. The large circle indicates the Sobolev-point along the line of sight, where $w_{prof} = \mu w(x)$ is the velocity or frequency in the profile for which the flux is calculated. (*a*) Integration scheme for a singlet at a wavelength shortward of the rest wavelength (i.e., $w_{prof} < 0$). (*b*) Integration points for a doublet with a small separation, at a wavelength shortward of the rest wavelength of both components. The Sobolev-points where $(\mu w)_B = w_{prof}$ and $(\mu w)_R = w_{prof} - \delta$ are shown by large circles. Small circles indicate the integration where the red line contributes; vertical marks indicate where the blue line contributes to the τ and I integrals. (*c*) Integration points for a doublet with large separation, at a wavelength w_{prof} between the rest wavelengths of the two components. The symbols same as in (*b*).

tion, with the exception that we allow for the possible existence of photospheric absorption components. The equation of radiative transfer is solved exactly.

a) The Source Function

In the previous section we argued that the source function of the blue component will not be altered by the presence of the red component. So, the source function is identical to the one described in § III*a*:

$$S_B(x_B) = [\beta_{c_B} I^* + \epsilon'_B B(x_B)]/(\beta_B + \epsilon'_B) . \quad (21)$$

(For simplicity we have omitted the subscript v.) The escape probabilities are the same as in equations (5) and (6) or (13), with the exception that τ_0 should be replaced by τ_{0_B}, which is the optical depth of the blue component.

The source function of the red component at x_R is

$$S_R(x_R) = [(\bar{\beta}_{c_R} I^* + c_R) + \epsilon'_R B(x_R)]/(\beta_R + \epsilon'_R) , \quad (22)$$

where

$$\bar{\beta}_{c_R}(x_R) = \frac{1}{2}\int_{\mu_c}^{1} \exp\,[-\tau^B(x_B, \mu_B)] \times \left\{\frac{1 - \exp\,[-\tau^R(x_R, \mu_R)]}{\tau^R(x_R, \mu_R)}\right\} d\mu_R \quad (23)$$

and

$$c_R(x_R) = \tfrac{1}{2}\int_{-1}^{1} S_B(x_B)\{1 - \exp\,[-\tau^B(x_B, \mu_B)]\} \times \{1 - \exp\,[-\tau^R(x_R, \mu_R)]\}/\tau^R(x_R, \mu_R) d\mu_R . \quad (24)$$

In these expressions the optical depth is

$$\tau^R(x_R, \mu_R) = \tau_{0_R}/(1 + \sigma^2\mu_R) , \quad (25)$$

and similarly for τ^B.

The first term of the source function S_R (eq. [22]) is the contribution to the mean intensity by the photospheric radiation. Since this radiation can be reduced by the absorption in the blue component, the expression for $\bar{\beta}_{c_R}$ differs from the one in the single-line case (eq. [6]) by the factor exp $(-\tau^B)$. The second term describes the contribution to the mean intensity at x_R by the radiation from the blue component, which is of the form $S_B(1 - e^{-\tau_B})$. The third term is the emission generated locally at x_R.

The expressions for $\bar{\beta}_{c_R}(x_R)$ and $c_R(x_R)$ contain the coordinate x_B and the angle μ_B. For each x_R and μ_R one has to find the point in the wind from where the photons emitted by the blue component can be absorbed by the red component at x_R. This "radiatively coupled point" is described by its distance x_B from the star and the angle μ_B which defines the direction to the point x_R. This is shown schematically in Figure 3. The conditions for radiatively coupled points are

$$\mu_R\, w(x_R) - \mu_B\, w(x_B) = \delta , \quad (26)$$

$$x_R(1 - \mu_R^2)^{1/2} = x_B(1 - \mu_B^2)^{1/2} , \quad (27)$$

provided that the line between the two radiatively coupled points does not cross the star. For those values of x_R and μ_R for which no radiatively coupled points exist, the value of τ_B in equations (23) and (24) should be set to zero.

If the photosphere does not emit a continuum, but its spectrum has absorption lines centered at v_{0_B} and v_{0_R}, the expressions β_{0_B} and $\bar{\beta}_{c_R}$, which described the contributions by the photospheric radiation, will be modified. Suppose that the absorption lines are given by expressions similar to equation (11) with A_B, v_{0_B} and A_R, v_{0_R} for the blue and red component respectively. In that case the integrands of β_{c_B} and $\bar{\beta}_{c_R}$ should be multiplied by $1 - A_B(\Delta v'_B)$ and $1 - A_R(\Delta v'_R)$ respectively, in a similar way as in equation (13) for a single line. The term c_R also contains a contribution from photospheric radiation scattered via the blue component to the red component. However, the effect of the photospheric absorption line in this term is automatically allowed for by the reduction of S_B due to β_{c_B}. So the expression for c_R is not affected by the presence of a photospheric absorption line.

b) The Solution of the Transfer Equation

The solution of the transfer equation in the case of doublets goes essentially in the same way as in the case of singlet. At any frequency v the intensity emerging from a line of sight, specified by p, is

$$I_v(p) = \int_{-\infty}^{\infty} [S_B(z')\kappa_B(z') + S_R(z')\kappa_R(z')]e^{-\tau_v(z')}dz' , \quad \text{for } p \geq 1 , \quad (28)$$

and

$$I_v(p) = \int_{-\infty}^{-z_*} [S_B(z')\kappa_B(z') + S_R(z')\kappa_R(z')] \times e^{-\tau_v(z')}dz' + I_v^* e^{-\tau_v(-z_*)} , \quad \text{for } p < 1 . \quad (29)$$

In these expressions the absorption coefficient $\kappa_B(z')$ is

$$\kappa_B(z') = \tau_0^B(x)\Phi_v^B(z')/[1 + \sigma(x)(z'/x)^2] , \quad (30)$$

where $x = (p^2 + z'^2)^{1/2}$. The expression for $\kappa_R(z')$ is similar. The profile function Φ should be calculated at the point z' where the Doppler shift is calculated for the blue and red component. So

$$\Phi_v^B(z') = \phi(\Delta w_B)dw_z/dz , \quad (31a)$$

$$\Phi_v^R(z') = \phi(\Delta w_R)dw_z/dz , \quad (31b)$$

with

$$\Delta w_B = \left(\frac{z'}{x}\right)w(x) - \left(\frac{v - v_0^B}{v_0^B}\right)\frac{c}{v_\infty} \quad (32)$$

and

$$\Delta w_R = \Delta w_B + \delta . \quad (33)$$

We assume that the intrinsic absorption profile ϕ of the red and the blue component is the same. The optical depth $\tau_v(z')$ in equations (28) and (29) is defined by

$$\tau_v(z') = \int_{-\infty}^{z'} [\kappa_B(\zeta) + \kappa_R(\zeta)]d\zeta , \quad (34)$$

where ζ is the z-coordinate along a line of constant p.

If the photosphere emits a continuum with absorption lines at v_{0_B} and v_{0_R}, the factor I^* in equation (29) should be reduced by $(1 - A_v)$, where A_v is the absorption.

The flux F_v is found by integrating I_v over p, as in equation (19). The integration scheme for the calculation of I is shown in Figure 2.

c) Tests for Some Limiting Cases

It is useful to test the expressions derived for the source functions and the intensities of doublets in some limiting cases,

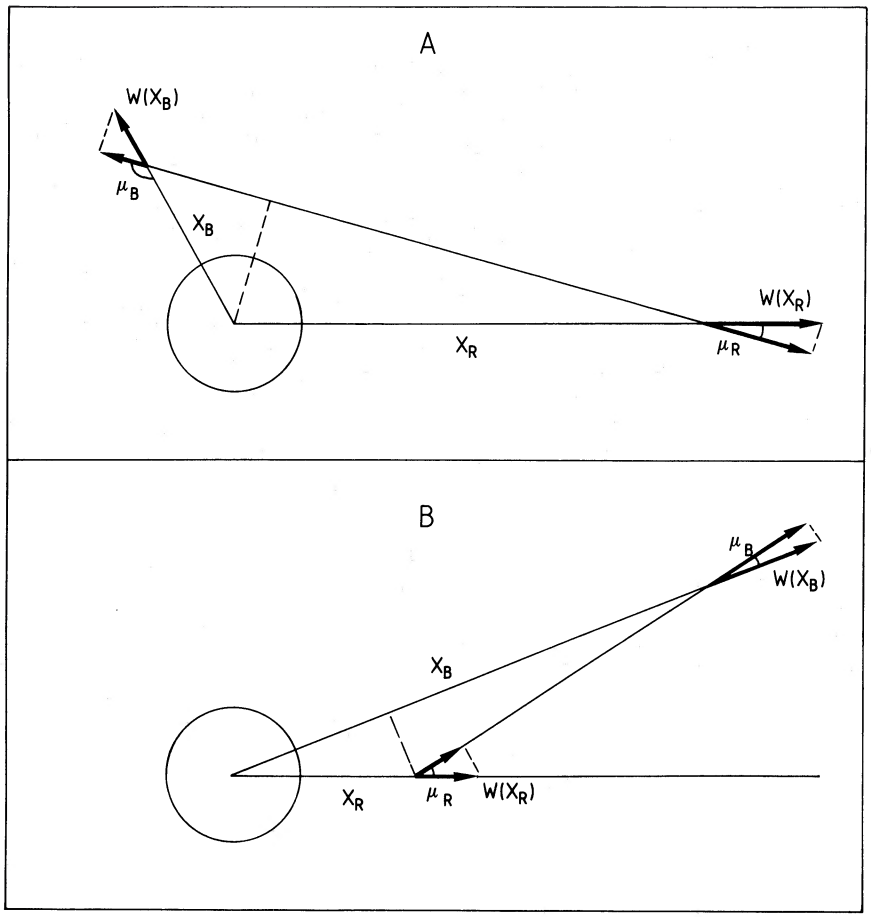

FIG. 3.—Two cases of radiatively coupled points located at x_R and x_B, which satisfy the conditions given by eqs. (27) and (26).

e.g., when the doublet reduces to a singlet and when the separation between the two components is either very large or very small. The last case especially is not trivial, and we discuss the consequences.

i) *One Line Only*: $\tau^R = 0$ *or* $\tau^B = 0$

In this case there are no radiatively coupled points, so $c_R = 0$. Equations (28) and (29) reduce the same expressions as for a single line. If $\tau^B = 0$, the resulting single line will be shifted to the red by a velocity δ, as expected.

ii) *Doublet Separated by* $\delta > 2$

In this case the two components do not interfere with one another, and equations (28) and (29) reduce to those of two individual lines, separated by δ, as expected.

iii) *Doublets Separated by* $\delta = 0$

In this case the two components are expected to act as one line, with an opacity equal to the sum of the two. At any point in the atmosphere and for any direction μ, the ratio $\kappa_R/\kappa_B = K$ and $\tau_R/\tau_B = K$ is a constant $K = \tau_0^R/\tau_0^B$. We can see from equations (28) and (29) that the two components will act as one line of combined opacity if $S_B(x) = S_R(x)$. This, however, is not the case in our expressions for the source functions (21) and (22). For instance, the expressions for β_{c_B} and $\bar{\beta}_{c_R}$ are different, as well as those for β_B and β_R. This is true even if we consider the fact that the radiatively coupled points which enter into the calculation of c_R and $\bar{\beta}_{c_R}$ and which satisfy equations (26) and (27) always coincide, so $x_R = x_B$ and $\mu_R = \mu_B$. Then in this case our formalism is not applicable. The physical reason for this breakdown is the invalidity of our assumption that the source function of the blue component is unaffected by the red component. This condition is obviously not maintained if the two components are so close together that their frequencies are within the width of one another's intrinsic absorption profile.

From these considerations we expect that our method for calculating the source function of doublets will produce significant errors for those cases in which the separation of the components is small or of the same order as the intrinsic width of the profiles. If the intrinsic profile has a Gaussian shape with a Doppler width w_D, in terms of the normalized velocity, the SEI method will give significant errors if $\delta \leq 2w_D$. For smaller separations of $\delta < w_D$, the source function can be better calculated by assuming that it refers to a singlet with the sum of the two opacities. The transfer equation can still be solved exactly.

V. COMPARISON WITH OTHER METHODS

In this section we describe some results and compare them with profiles calculated by other methods. In particular, the profiles are compared with those predicted by the escape probability method (EP; Castor 1970), which uses the Sobolev approximation in the calculation of both the source function and the intensities; and with those predicted with the more accurate comoving frame method (CF; Hamman 1980). Our method, SEI, has an accuracy between these two, since it uses the Sobolev source functions but the exact integration of the

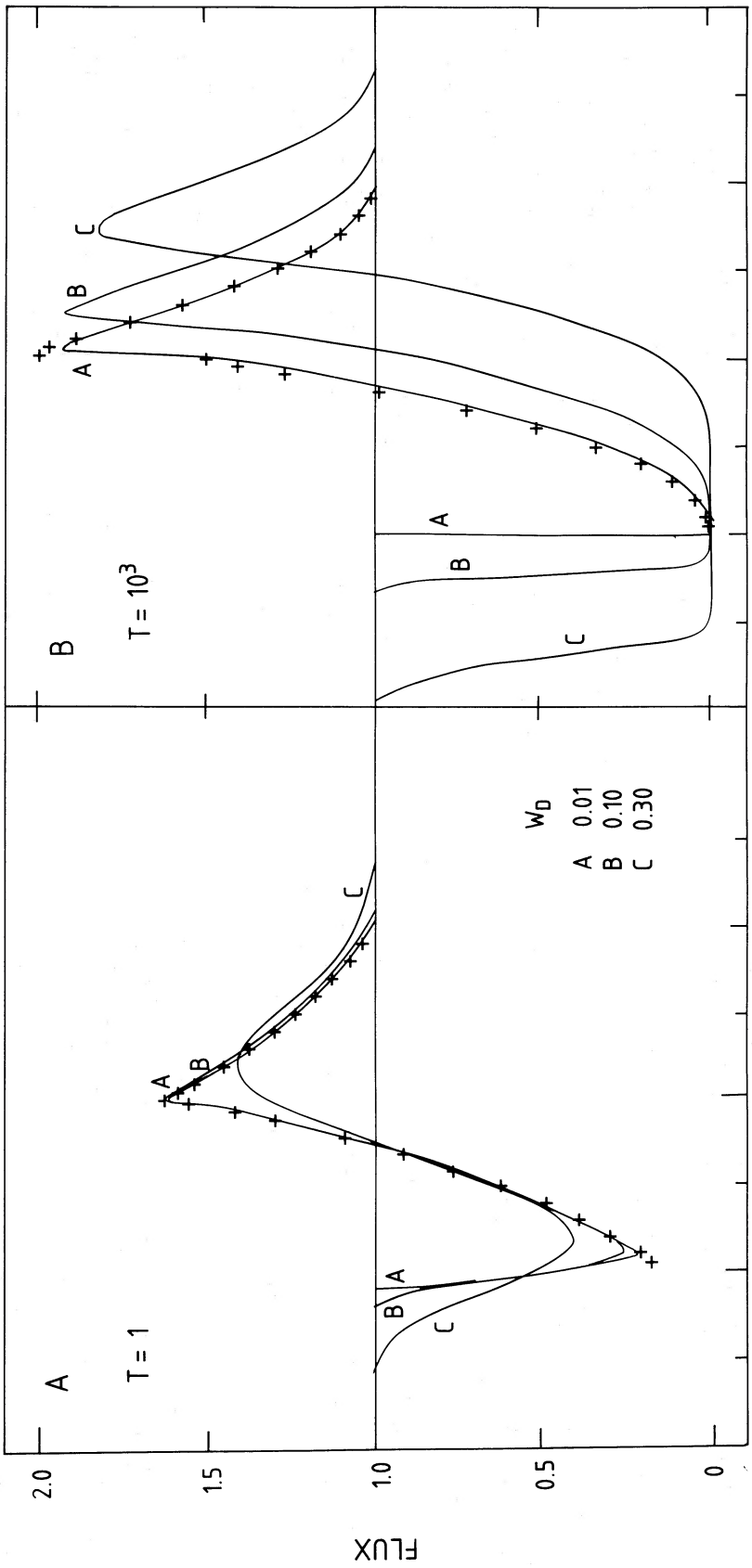

FIG. 4.—Comparison between profiles calculated with the Sobolev approximation (*pluses*) and with the SEI method (*solid lines*) for three values of the turbulent velocity w_D normalized to v_∞. The total optical depth is (*a*) $T = 1$ and (*b*) $T = 1000$. Note the drastic variations in the profiles if $w_D \geq 0.1$. The edge velocity of the strong lines is increased by $\sim 2w_D$.

transfer equations. We expect the results to be quite similar to those of the CF method.

a) Comparison with the Escape Probability Method

In Figure 4 a set of profiles calculated with the EP method, published by Castor and Lamers (1979), are compared with profiles with the SEI method. In both cases the velocity law is assumed to vary as

$$w(x) = w_0 + (1 - w_0)(1 - 1/x)^{\beta}, \quad (35)$$

with $\beta = 1$ and $w_0 = 0.01$. The optical depth is parameterized by

$$\tau_1(w) = T(\gamma + 1)(1 - w_0)^{-1-\gamma}(1 - w)^{\gamma}, \quad (36)$$

where $\tau_1(w)$ is defined by

$$\tau_1(x) = (\pi e^2/mc) f \lambda_0 n_i (dr/dv) = \tau_0(x)(d \ln x/d \ln w) \quad (37)$$

(see eq. [9]). These expressions were adopted by Castor and Lamers (1979), because they give line profiles which resemble the observed profiles of UV resonance lines in hot stars, if $\gamma \approx 1$ or 2 (see, e.g., Gathier, Lamers, and Snow 1981; Garmany *et al.* 1981).

The profiles in Figure 4 show two cases, large and small optical depth $T = 10^3$ and $T = 1$. The EP profiles are compared with SEI profiles with a Gaussian turbulence with a Doppler width $w_D = 0.01$, 0.1, and 0.3.

The profiles in Figure 4*a* show the effect of the turbulence on the profile of an unsaturated line. In the case of a very small turbulent velocity, $w_D = 0.01$, the profile is very similar to the one calculated with the Sobolev approximation. An increase in the turbulent velocity has the following effects: (*a*) the absorption part of the profile becomes wider and shallower; (*b*) the transition from absorption into emission shifts to the red; (*c*) the height of the emission peak decreases and shifts to the red. The profiles in Figure 4*b* show the effect of turbulence on a saturated line. The increase of turbulence shifts the violet absorption wing to shorter wavelengths. The half-depth is shifted with respect to v_∞ by $\sim -2w_D$. At the same time the emission peak shifts to the red by $\sim +2.5w_D$. The first effect will result in an overestimate of the terminal velocity of a wind by about twice the turbulent velocity at a large distance from the star, where v approaches v_∞. The second effect produces an absorption which extends into the red part of the profile. If such a profile is interpreted with the Sobolev method, the presence of red absorption can only be explained by a strong underlying photospheric absorption component.

Both "errors" occurred in the first detailed analysis of the P Cygni profiles observed in the UV spectra of hot stars (Lamers and Morton 1976; Lamers and Rogerson 1978) and were discussed and "corrected" in the subsequent analysis of the same stars with the CF method by Hamann (1980, 1981*b*). (A description of the effect of the turbulence on the solution of the transfer equation has been given by Hamann 1981*a*, and will not be repeated here.)

b) Comparison with the Comoving-Frame Method

In Figures 5 and 6 a set of profiles calculated with the SEI method is compared with those of the CF method, published by Hamann (1981*a*). In this case Hamann's and our profiles are calculated for a wind with a velocity law

$$w(x) = (1 - 0.999/x)^{0.5} \quad (38)$$

and an optical depth law

$$\tau_1(w) = 2\kappa_0 w^{\alpha}, \quad (39)$$

where τ_1 is defined by equation (37). The turbulent velocity is $w_D = 0.1$.

The results of single lines are shown in Figure 5, for the case of $\alpha = -3$, 0, and 2. The agreement between our results and those calculated with the CF method is very good. Only minor differences are seen, mainly as a small underestimate of the amount of emission for the strongest lines. This result was already predicted by Hamann (1981*a*). The small absorption dip at $w \approx 0.2$ in our profiles of $\alpha = -3$ is due to a numerical effect, because we started the integration of the transfer equation at $x = 1.001$ instead of 1. We conclude that the SEI profiles of single lines are very similar to those calculated with the CF method.

In Figure 6 we show the results for the case of doublet lines calculated for the same velocity law and optical depth law as before, with $\alpha = 0$. The separation of the doublet is assumed to be 0.7, and the turbulent width is $w_D = 0.1$. The top figure shows the case of $\kappa_0^B = 0.5$ and $\kappa_0^R = 0.25$, whereas the lower figure is for $\kappa_0^B = 10$ and $\kappa_0^R = 5$.

We see that the agreement between the two methods is very good except for the slight underestimate of the peak of the emission.

From the comparison between the profiles of single lines and doublets calculated with our method and the CF method, we conclude that the profiles computed with our method have an accuracy similar to that of the CF method.

VI. RESULTS OF THE SEI METHOD

In this section we describe some results obtained with our method and show some characteristic profiles obtained for various physical conditions in the wind.

a) Adopted Physical Quantities

The velocity law is described by equation (35). For all cases we assume $w_0 = 0.01$ and $\beta = 1$. These parameters predict velocity laws which are in reasonable agreement with those derived from the UV resonance lines of hot stars (see, e.g., Gathier, Lamers, and Snow 1981).

We have chosen to express the opacity in terms of $\tau_1(w)$, defined in equation (37). The reason for this choice is that the absorption part of the P Cygni profiles depends strongly on $\tau_1(w)$, which was shown by Castor and Lamers (1979). (In fact, for the violet part of the profile, well outside the line center, the flux is on the order of $e^{-\tau_1}$). Since $\tau_1(w) \propto n_i(dx/dw)$, $dx/dw \propto x^2 w^{1/\beta - 1}$ and $n_i \propto x^{-2} w^{-1} q_i$, where q_i is the ionization fraction of the observed ion, one expects that $\tau_1(w) \propto w^{(1/\beta)-2} q_i$. If the ionization balance is dominated by photoionizations and radiative recombinations in an optically thin wind ($J_\nu \propto x^{-2}$ and $n_e \propto x^{-2} w^{-1}$), the ionization fraction will vary approximately as $q_i \propto w^{i-m}$, where i is the ionization stage of the observed ion and m is the ionization stage of the ion in the dominant stage of ionization ($q_m = 1$). So in this case one might expect $\tau_1(w) \propto w^n$ with $n = \beta^{-1} - 2 + i - m$. For instance, if CV were the dominant stage of ionization in a wind which has a velocity law described by $\beta = 1$, the optical depth of the C IV resonance lines is expected to vary as $\tau_1 \propto w^{-1}$ and the C III resonance lines as $\tau_1 \propto w^{-2}$. If the ionization fraction varies as $x^{-s} w^{-t}$, the optical depth will vary approximately as $\tau_1 \approx w^{\alpha_1}(1 - w^{1/\beta})^{\alpha_2}$, with $\alpha_1 = \beta^{-1} - 2 - t$ and $\alpha_2 = +s$. The

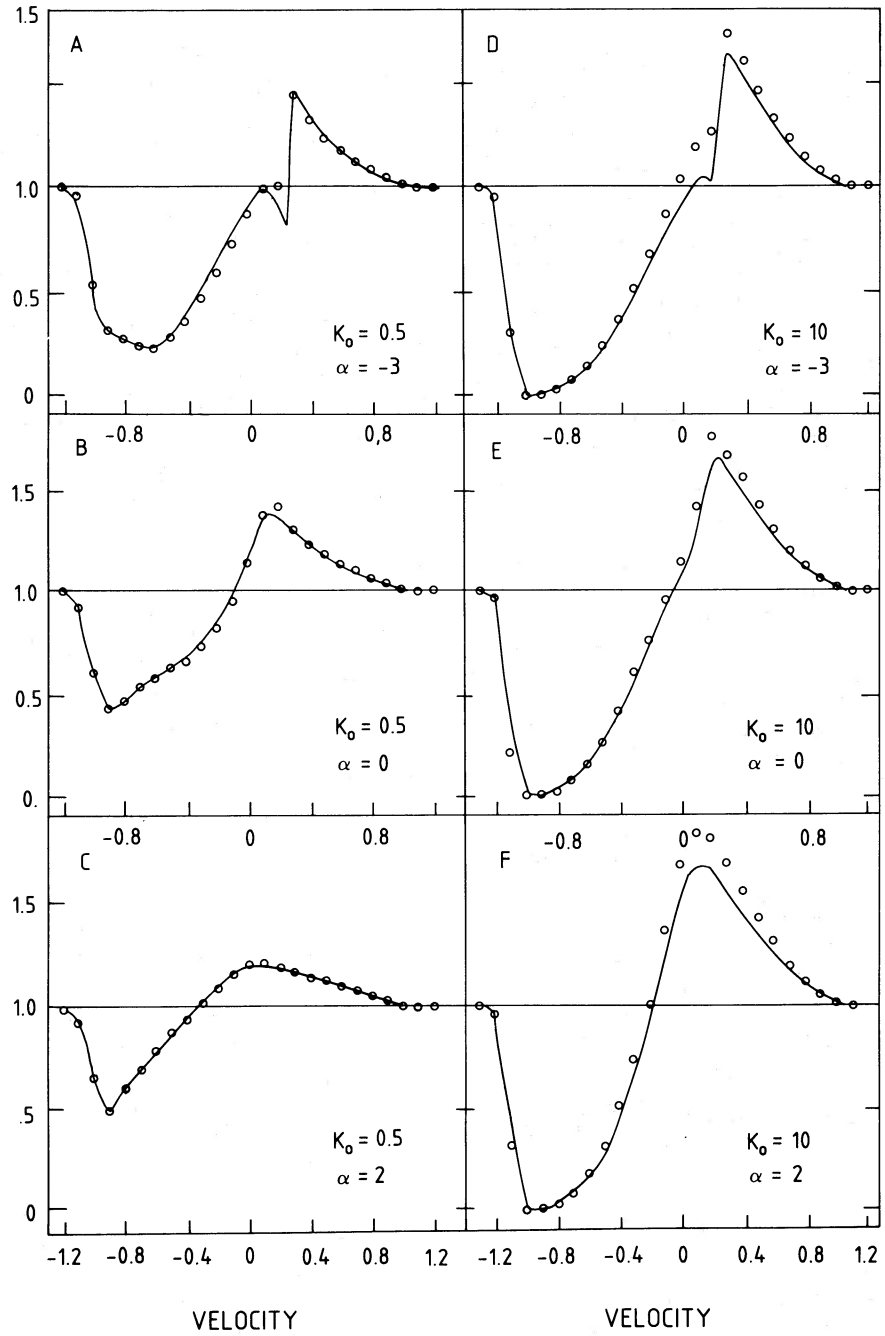

FIG. 5.—Comparison between profiles calculated with the comoving frame method (*circles*) and with the SEI method (*solid lines*). The figure shows (*a*)–(*c*) several optically thin lines and (*d*)–(*f*) thick lines, with parameters given in § V*b*. The SEI method understimates the amount of emission by a small factor. The dip in the SEI profiles of (*a*) and (*d*) is due to numerical effect in the integration of I, which was started at $x = 1.001$ for the SEI profiles and at $x = 1$ for the CF profiles. The CF profiles are from Hamann (1981*a*).

observed profiles in the UV spectra of O and B stars can indeed be fitted by assuming an optical depth law of this type (e.g., Lamers and Morton 1976; Gathier, Lamers, and Snow 1981; Garmany *et al.* 1981).

In the UV spectra of some stars the violet wings of several P Cygni profiles do not extend to v_∞ or to $w = 1$, but to a smaller velocity $w_1 < 1$. These can be represented by profile calculations in which τ_1 is specified as a function of w/w_1 instead of w (see, e.g., Lamers and Morton 1976).

In order to have our program as versatile as possible, τ_1 is specified as a combination of the cases described above:

$$\tau_1(w) = (T/I)(w/w_1)^{\alpha_1}[1 - (w/w_1)^{1/\beta}]^{\alpha_2}\,, \tag{40}$$

where

$$I = w_1 \int_{w_0/w_1}^{1} y^{\alpha_1}(1 - y^{1/\beta})^{\alpha_2} dy\,. \tag{41}$$

In these expressions T, α_1, α_2, and w_1 are the free parameters.

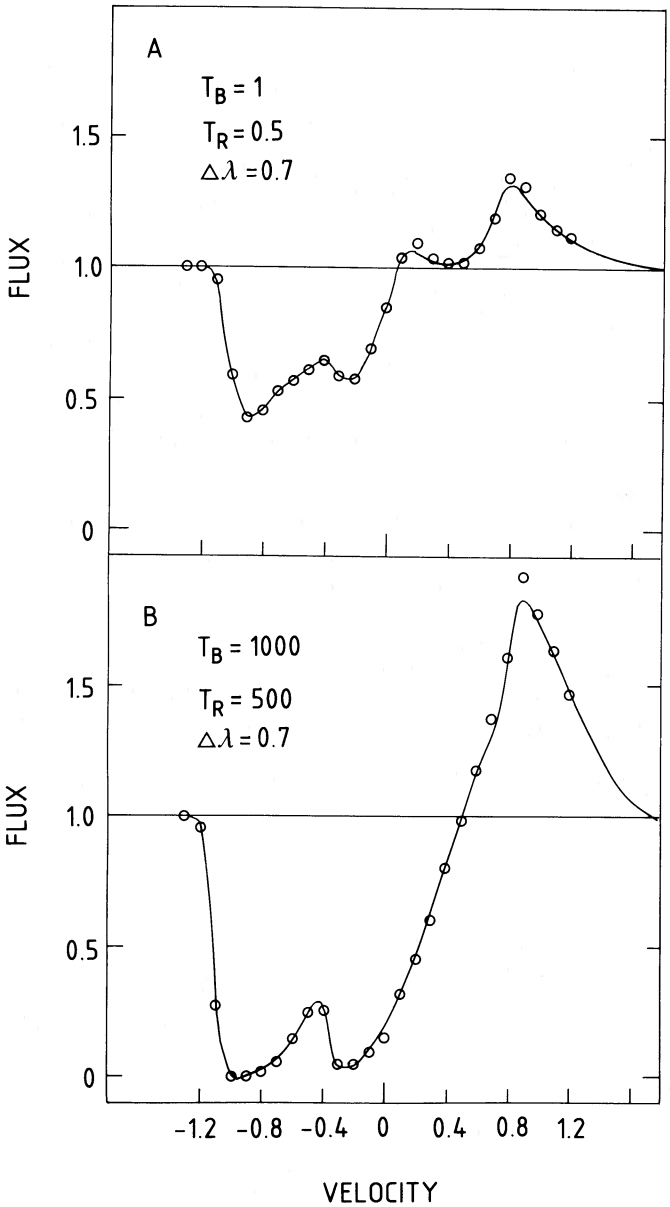

FIG. 6.—Comparison of the profiles of a doublet with separation $\delta = 0.7$ and a turbulent velocity of $0.1v_\infty$ calculated with the comoving frame method (*circles*) by Hamann (1981*a*) and with the SEI method (*solid lines*). (*a*) Case of an optically thin line; (*b*) thick line. Note the excellent agreement, apart from a small underestimate of the height of the peak of the emission by the SEI method.

If the observed P Cygni profile extends its violet absorption to v_∞, then $w_1 = 1$. The parameter T is the integrated optical depth between $x = 1$ and $x = \infty$. In the case of resonance lines, when the population of the upper levels can be neglected (eq. [37]), T is related to the column density N_i of the observed ion

$$T = (\pi e^2/mc) f\lambda_0 N_i/v_\infty \, . \tag{42}$$

The source function contains a parameter $\epsilon' = C_{21}/A_{21}$, which has to be specified in our program. The collisional de-excitation rate can be approximated by

$$C_{21} \approx 1.7 \times 10^{-3} f T_e^{-1/2} \chi_{eV}^{-1} n_e (g_1/g_2) P(\chi/kT_e) \tag{43}$$

(Allen 1963, p. 43), where χ_{eV} and χ are the excitation energies of the upper level in eV and in ergs respectively, and P is a slowly varying function. So to a first-order approximation we can expect that $\epsilon' \propto n_e T_e^{-1/2} \propto x^{-2} w^{-1} T_e^{-1/2}$. Ignoring the temperature dependence, we have expressed ϵ' as

$$\epsilon' = \epsilon'_0 \, w_0/x^2 w \, , \tag{44}$$

where $\epsilon'_0 = \epsilon'(x = 1)$. For a star with $R/R_\odot \approx 5$, $T = 50{,}000$ K, $\dot{M} \approx 10^{-7} \, M_\odot \, \mathrm{yr}^{-1}$, and a wind velocity of 30 km s^{-1} at $x = 1$, ϵ'_0 is on the order of 10^{-5} both for resonance lines and for lines excited levels at $1000 < \lambda < 1500$ Å.

The collisional term in the source function, $\epsilon' B_\nu$, requires the specification of the Planck function and its variation with distance or velocity in the wind. We express the Planck function in terms of the continuum intensity I_c, so that all intensities and fluxes are relative to the continuum. In the program the following parameterization for B_ν has been adopted:

$$B_\nu/I_c = (B_\nu/I_c)_0 \exp\left[-a_T(w - w_0)\right] \, , \tag{45}$$

where $(B/I_c)_0$ is its value at $x = 1$ and $w = w_0$. An isothermal wind is represented by $a_T = 0$; a positive value of a_T corresponds to a Planck function which decreases outwards to about a factor e^{-a_T} of its initial value, and a negative value of a_T implies an increase by a factor exp ($|a_T|$).

The profiles were calculated with the parameterization of $w(x)$, $\tau_1(w)$, $\epsilon'(x)$, and $B_\nu(w)$ as described above. These parameterizations can easily be changed in the program, if required.

b) Some Resulting Profiles

In this section we show and discuss some profiles obtained with our program. All profiles were calculated for a velocity law described by equation (35) with an initial velocity $w_0 = 0.01$ and $\beta = 1$, and with a constant optical depth; $\alpha_1 = \alpha_2 = 0$ in equation (40).

Figure 7 shows the profiles from an isothermal wind ($a_T = 0$ in eq. [45]) with various values of the collisional term $\epsilon' B_\nu$ in the source function (eq. [4]). This term varies as

$$\epsilon' B_\nu/I_c = \epsilon'_0 (B_\nu/I_c)_0 (w_0/x^2 w) \, , \tag{46}$$

where $\epsilon'_0(B_\nu/I_c)$ is a free parameter. The profiles are calculated for a turbulent velocity of $w_D = 0.1$ and 0.25 and with $10^{-1} \geq \epsilon'_0(B_\nu/I_c)_0 \leq 10^3$, for a total optical depth of $T = 1$. We see that, as the value of $\epsilon'_0(B_\nu/I_c)_0$ increases, the profile varies from a normal P Cygni profile (Figs. 7*a* and 7*b*) to an emission profile with a violet absorption component (Figs. 7*c* and 7*d*) and finally to a round emission profile at $\epsilon'_0(B_\nu/I_c)_0 \geq 10^3$. The profiles of the type shown in Figures 7*a* and 7*b* resemble those observed in the UV spectrum of luminous supergiants. Profiles like the one in Figure 7*d* resemble those observed in the UV spectrum of the Wolf-Rayet stars. They have a typical Gaussian-shape emission. Note that the emission is slightly asymmetric and its center is shifted to the red, while the absorption is shifted to the blue.

Figure 8 shows a set of profiles calculated with a large optical depth $T = 10^3$ and $10^{-3} \leq \epsilon'_0(B_\nu/I_c)_0 \leq 10$. In this case the violet absorption always reaches zero. The profiles vary again from P Cygni profiles for small collisional terms to very strong round emission profiles for large collisional terms. Note that in this case the emissions are almost symmetrical but that they are strongly redshifted, by ~ 0.25 if $w_D = 0.10$ and by ~ 0.65 if $w_D = 0.25$. So the shift is ~ 2.5 times the turbulent velocity.

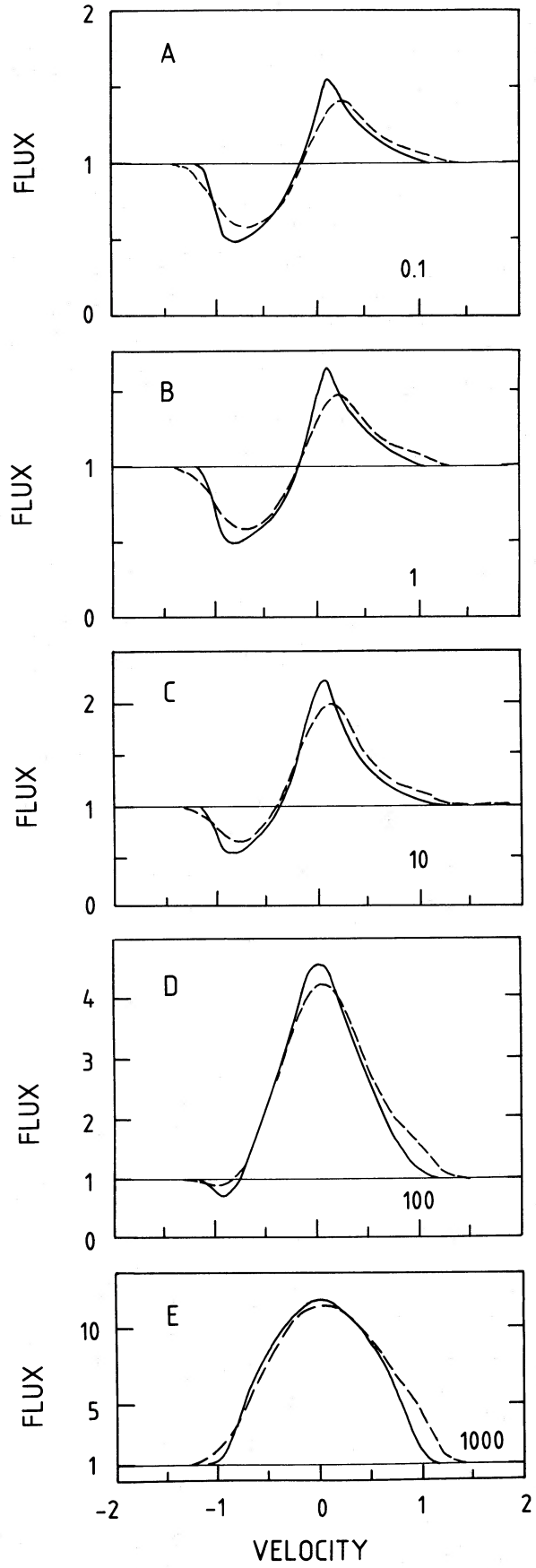

Figure 9 shows some profiles calculated for winds with different temperature structures: a temperature which decreases outward by a factor of 0.05 ($a_T = +3$ in eq. [45]), isothermal wind ($a_T = 0$), and a temperature which increases by a factor of 20 ($a_T = -3$). The profile with $a_T = +3$ resembles the one with constant temperature and $\epsilon'_0(B_\nu/I_c)_0 \approx 10$, as shown in Figure 7*c*, and the one with $a_T = -3$ resembles the profile with constant temperature and $\epsilon'_0(B_\nu/I_c)_0 \approx 2000$ [twice as high as the one in Fig. 7*e* with $\epsilon'_0(B_\nu/I_c)_0 = 1000$]. This is due to the fact that the emission is dominated by contributions formed at a distance of $x \geq 2$ from the star. So the emission is sensitive to the value of $\epsilon' B_\nu$ reached at a distance where the velocity is $0.5 \leq w \leq 1$, with $\epsilon' B_\nu \sim 5$–10 in the first profile, 100 in the second one, and 1000–2000 in the third one. We conclude that an outward decrease or increase of the temperature can be mimicked in the profiles by assuming a lower or a higher mean temperature (or ϵ') in the calculation of the collisional term in the source function. This implies that the profile of an emission line in the spectra of Wolf-Rayet stars gives little information on the variation of the temperature in their winds and provides only an estimate of the *mean* temperature at a distance of $x \geq 2$.

VII. SUMMARY AND DISCUSSION

In this paper we have described a new method for calculating line profiles formed in spherically symmetric stellar winds in which the velocity increases monotonically outward. The source function is calculated with the escape probability method, but the transfer equation is solved exactly. This results in a method which in many cases reaches the same accuracy as the profiles calculated with the comoving-frame method (Mihalas, Kunasz, and Hummer 1975; Hamann 1981*a*) but has the advantages of the escape probability method. It can be run on a small computer and requires little CPU time, so that it can be used in an interactive analysis of observed line profiles.

The method has a disadvantage compared to the CF method. The photospheric spectrum is taken as a lower boundary of the transfer equation, so that the transition from the photosphere to the wind is not properly taken into account. This may produce errors in the profiles near the line center. However, in those cases where the wind velocity is much larger than the photospheric velocity, this imperfection will not hamper the analysis of the observations. Moreover, at present our knowledge about the structure and velocity of the upper photosphere/lower wind layers is very limited, so that profiles which are reliable close to the line center cannot be calculated anyway. If one wants to derive information about these lower wind layers from the observed line profiles, the CF method has to be used.

The profiles calculated with our method are compared with those obtained with the escape probability method and with the comoving frame method in §§ V*a* and V*b* respectively. The first comparison shows the drastic changes to the line profiles if chaotic motions in the winds are taken into account (see Fig. 4). These motions, called "turbulence" for simplicity, tend

FIG. 7.—Some profiles calculated with the SEI method for lines of the same velocity law in the wind and the same optical depth law $\tau_1(w)$, but with increasing collisional terms in the source function. The total optical depth $T = 1$. The value of the collisional parameter $\epsilon'_0(B_\nu/I_c)_0$ is indicated in the figures. The turbulent velocity is $0.1v_\infty$ (*solid lines*) or $0.25v_\infty$ (*dashed lines*). For large values of the collisional parameter the lines approach symmetric emission profiles, with the emission slightly shifted to the red.

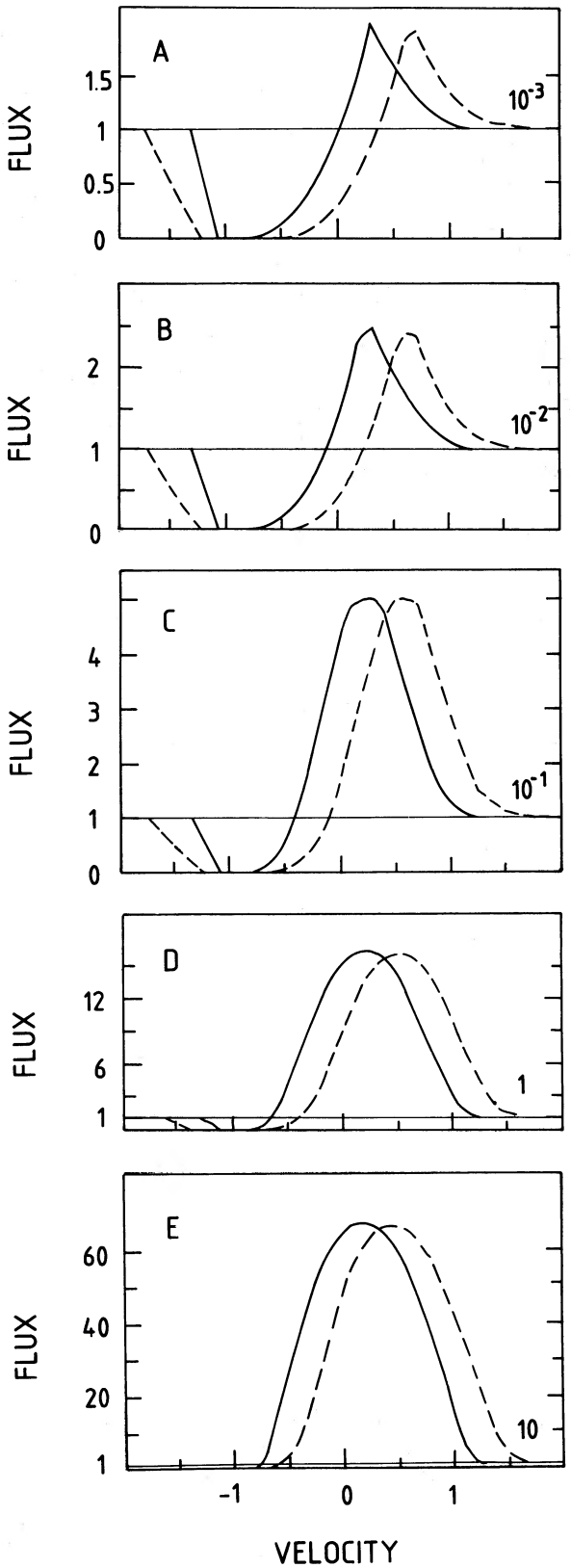

FIG. 8.—Profiles of the same lines as in Fig. 7, but with a total optical depth $T = 1000$. In this case the shift of the emission component to the red by ~ 2.5 times the turbulent velocity is clearly visible in the profiles, as well as the widening of the absorption component. The value of the collisional parameter is indicated in the figures.

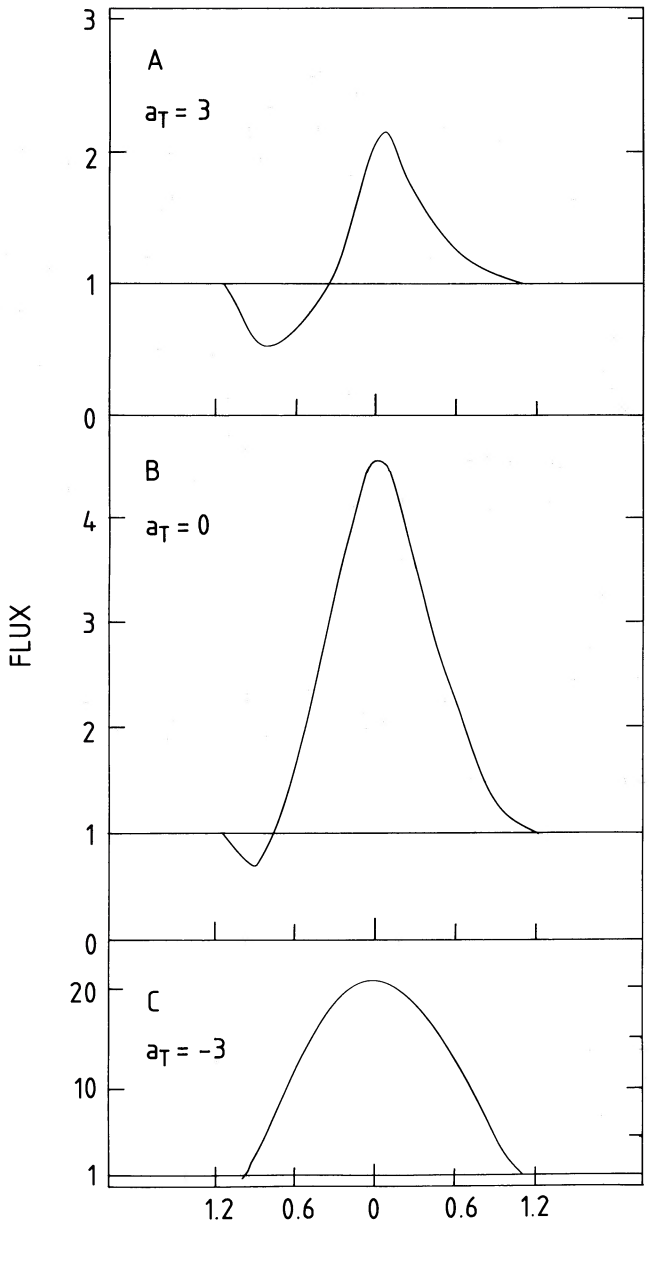

FIG. 9.—Profiles of lines with an appreciable collisional contribution to the source function formed in winds of different temperature structure, described by eq. (45). The temperature (*a*) decreases outward, (*b*) is constant, and (*c*) increases. The total optical depth is $T = 1$, and the collisional parameter is $\epsilon'_0(B_\nu/I_c)_0 = 100$. Note the very large differences in the profiles.

to shift the absorption edge of the P Cygni profiles to the violet (which results in an overestimate of the terminal velocities of the wind) and the emission component to the red. This second effect, if not propertly taken into account, may be erroneously taken for the presence of a strong photospheric absorption component (see also Hamann 1981*a* and Bertout 1984). If the turbulent velocity is small, $w_D \lesssim 0.02$, the profiles calculated with our SEI method are identical to those calculated with the Sobolev method.

The comparison between the profiles of our method with those calculated by the CF method (Hamann 1981*a*) shows a

very good agreement for both optically thin and optically thick lines (Fig. 5). For optically very thick lines, our method underestimates the emission peak by $\sim 10\%$. Also in the case of doublets, our profiles are very similar to those calculated with the CF method.

We conclude that the SEI method for calculating line profiles in stellar winds is very efficient and accurate. Because of the simplicity and speed of the SEI program, it can be used for interactive analysis of stellar spectra on a medium (VAX-type) or minicomputer.

The program has been developed on a VAX 750 computer. A BASIC version, which can be run on an IBM or Olivetti (M24) personal computer, has also been developed. The Fortran program and ist numerical methods will be described in a forthcoming paper in *Computer Physics Communications.*

H. J. G. L. M. L. wishes to thank Dr. F. Pacini for financial support and hospitality at the Osservatorio Astrofisico di Arcetri during three brief periods in 1984 and 1985. We thank J. Cassinelli, R. Rutten, A. Hearn, and D. Hummer for useful comments on the paper, and L. Haas for typing the manuscript.

REFERENCES

Allen, C. W. 1963, *Astrophysical Quantities* (London: Athlone).
Bertout, C. 1984, *Ap. J.*, **285**, 269.
Castor, J. I. 1970, *M.N.R.A.S.*, **149**, 111.
Castor, J. I., and Lamers, H. J. G. L. M. 1979, *Ap. J. Suppl.*, **39**, 481.
Conti, P. S., and Garmany, C. D. 1980, *Ap. J.*, **238**, 190.
Garmany, C. D., Olson, G. L., Conti, P. S., and van Steenberg, M. E. 1981, *Ap. J.*, **250**, 660.
Gathier, R., Lamers, H. J. G. L. M., and Snow, T. P. 1981, *Ap. J.*, **247**, 173.
Hamann, W.-R. 1980, *Astr. Ap.*, **84**, 342.
———. 1981*a*, *Astr. Ap.*, **93**, 353.
———. 1981*b*, *Astr. Ap.*, **100**, 169.
Lamers, H. J. G. L. M., and Morton D. C. 1976, *Ap. J. Suppl.*, **32**, 715.
Lamers, H. J. G. L. M., and Rogerson, J. B. 1978, *Astr. Ap.*, **66**, 417.
Mihalas, D. 1978, *Stellar Atmospheres* (San Francisco: Freeman).
Mihalas, D., Kunasz, P. B., and Hummer, D. G. 1975, *Ap. J.*, **202**, 465.
Olson, G. L. 1982, *Ap. J.*, **255**, 267.
Olson, G. L., and Castor, J. I. 1981, *Ap. J.*, **244**, 179.
Prinja, R. K., and Howarth, I. D. 1985, *Astr. Ap.*, **149**, 73.
Rybicki, G. B., and Hummer, D. G. 1978, *Ap. J.*, **219**, 654.
Surdej, J. 1980, *Ap. Space Sci.*, **73**, 101.

M. CERRUTI-SOLA: Osservatorio Astrofisico di Arcetri, Largo Enrico Fermi 5, 50125 Firenze, Italy

H. J. G. L. M. LAMERS: SRON Laboratory for Space Research, Beneluxlaan 21, 3527 HS Utrecht, The Netherlands

M. PERINOTTO: Istituto di Astronomia, Universitá di Firenze, Largo Enrico Fermi 5, 50125 Firenze, Italy